01 May 2000

Single Phase Flow Modeling in Packed Beds: Discrete Cell Approach Revisited

Y. Jiang

M. R. Khadilkar

M. (Muthanna) H. Al-Dahhan
Missouri University of Science and Technology, aldahhanm@mst.edu

M. P. Dudukovic

Recommended Citation

Y. Jiang et al., "Single Phase Flow Modeling in Packed Beds: Discrete Cell Approach Revisited," *Chemical Engineering Science*, vol. 55, no. 10, pp. 1829 - 1844, Elsevier, May 2000.
The definitive version is available at https://doi.org/10.1016/S0009-2509(99)00453-4

PERGAMON

Chemical Engineering Science 55 (2000) 1829–1844

Chemical Engineering Science

Single phase flow modeling in packed beds: discrete cell approach revisited

Y. Jiang, M.R. Khadilkar, M.H. Al-Dahhan*, M.P. Dudukovic

Chemical Reaction Engineering Laboratory (CREL), Department of Chemical Engineering, Washington University, Urbauer Hall 208, One Brookings Dr., St. Louis, MO 63130, USA

Received 14 June 1999; accepted 14 July 1999

Abstract

A discrete cell model (DCM), based on the minimization of the total rate of energy dissipation, is applied to compute the fluid velocity field in two-dimensional packed beds. The analysis of the individual terms of the energy dissipation rate equation is also presented. The results obtained by DCM are validated both by comparing them with the solutions of ensemble-averaged momentum and mass conservation equations (CFDLIB code) and by available experimental results. The differences between DCM and CFD simulations were found to be confined to within a 10% band over a wide range of Reynolds numbers ($Re' = 5$–171). Thus, a reasonable agreement between the predictions of the two methods can be claimed for engineering applications. An acceptable agreement of DCM/CFD predictions and the available experimental data in the literature is also achieved. The presented case studies justify the use of DCM for predicting the fluid velocity fields in packed beds with complex internal structures and with irregular distributed gas feeding points.

Keywords: Packed beds; Flow distribution; Internal structure nonuniformities; Discrete cell model (DCM); Minimization of energy dissipation rate; Computational fluid dynamics (CFD)

1. Introduction

Gas flow through packed beds is commonly encountered in industrial applications involving mass or/and heat transfer both with and without chemical reaction. Complete understanding of the gas flow distribution in packed beds is of considerable practical importance due to its significant effect on transport and reaction rates. It was shown that reaction and radial heat transfer can only be modeled correctly if the radial nonuniformities of the bed structure are properly accounted for (Lerou & Froment, 1977; Delmas & Froment, 1988; Daszkowski & Eigenberger, 1992). Therefore, over the years, a number of studies investigated the radial variation of the axial gas velocity in packed beds. This included axial velocity measurement at various radial positions, measurement of radial porosity profiles (Morales, Spinn & Smith, 1951; Schwartz & Smith, 1953; Benenati & Brosilow, 1962; Lerou & Froment, 1977; McGreavy, Foumeny & Javed, 1986; Stephenson & Stewart, 1986; Volkov, Reznikov, Khalilov, Zel'vensky, Yu & Sakodynsky, 1986; Peurrung, Rashidi & Kulp, 1995; Bey & Eigenberger, 1997), and modeling of the radial variation of axial velocity (Schwartz & Smith, 1953; Stanek & Szekely, 1972; Cohen & Metzner, 1981; Johnson & Kapner, 1990; Ziolkowska & Ziolkowski, 1993; Cheng & Yuan, 1997; Bey & Eigenberger, 1997; Subagyo, Standish & Brooks, 1998). It was noted, however, that in industrial packed beds, some nonuniformities either due to the presence of internal structures (Berninger & Vortmeyer, 1987a,b), or due to irregular gas inlet design (Szekely & Poveromo, 1975) could cause the flow not to be one-dimensional and the gas velocity to vary in both radial and axial direction. Such two-dimensional flow is called "non-parallel" flow in the literature (Stanek, 1994). Hence, for industrial applications of packed beds, it is certainly important to be able to effectively model the non-parallel gas flow. In general, three types of mathematical models have been developed for the treatment of non-parallel gas flow in packed beds. They are briefly summarized below.

It should be noted that our goal here is simulation and prediction of single-phase flow on a bed scale, i.e. the

* Corresponding author. Tel.: + 1-314-935-6082; fax: + 1-314-935-7211.

E-mail address: muthanna@wuche.wustle.edu (M.H. Al-Dahhan)

0009-2509/00/$ - see front matter
PII: S0009-2509(99)00453-4

Nomenclature

d_p	particle diameter (= 0.003), m
d_v	equivalent diameter of particle, m
D	width of model bed (= 0.072), 8 cells, m
E_1, E_2	Ergun constants ($E_1 = 150$; $E_2 = 1.75$)
$E_{v,j}$	mechanical energy dissipation rate in cell j, J/s (based on V_j)
$E_{v,\mathrm{bed}}$	total mechanical energy dissipation rate in the bed, J/s
$f_1, f_{1,j}$	resistance factor ($= 150(1-\varepsilon_j)^2\mu/(\rho\varepsilon_j^3\phi^2 d_p^2)$)
$f_2, f_{2,j}$	resistance factor ($= 1.75(1-\varepsilon_j)\rho/(\varepsilon_j^3\phi d_p)$)
H	height of model bed (= 0.288), 32 cells, m
N	total number of the cells ($8\times 32 = 264$)
N_c	number of cells in each row
p_0^k	pressure ($p_0^k - p$ non-equilibrium pressure)
P_c	pressure at the center of the cell, N/m^3
P_0	pressure, dyn/cm^2
P_z	pressure in the z direction, N/m^2
$\Delta P/\Delta Z$	pressure drop per unit cell length, N/m^3
r	radius of packed beds, m
Re'	Reynolds number, ($= V_0 d_p\rho/6/(\mu(1-\varepsilon_B))$)
Re_p	particle Reynolds number, ($= V_0 d_P\rho/\mu$)
S_i	cell face area at a given coordinate direction i, m^2
T_i	energy dissipation rate due to the inertial term, J/s
T_k	energy dissipation rate due to the kinetic term, J/s
T_v	energy dissipation rate due to the viscous term, J/s
u_0	material velocity, cm/s
$\mathbf{u}_k$	material k interstitial velocity ($\rho_k u_k \equiv \langle\alpha_k\rho_0 u_0\rangle$), cm/s
$\mathbf{u}'_k$	fluctuating part of material k interstitial velocity, cm/s
U_j	local interstitial velocity ($= V_j/\varepsilon_j$), m/s
U_0	input interstitial velocity ($= V_0/\varepsilon_B$), m/s
$\mathbf{V}$	velocity vector
$V_{c,j}$	volume of the cell j, ($= S_{z,j}\times\Delta Z$), m^3
V_j	superficial velocity in the jth cell, m/s
V_0	input superficial velocity, m/s
ΔZ, ΔX	size of the cell ($= 3d_p$), m

Greek letters

α_k	material indicator (= 1 if material k is present; = 0 otherwise)
$\dot{\alpha}_k$	material derivative
ε_B	bed porosity (= 0.415)
ε_j	porosity in the jth cell
θ_k	material k volume fraction ($\theta_k = \langle\alpha_k\rangle$)
μ	viscosity of fluid, Pa s (gas:1.8×10^{-5} Pa s; liquid:1.0×10^{-3} Pa s)
ρ	density of fluid, kg/m^3 (gas: 1.2 kg/m^3; liquid: 1000 kg/m^3)
ρ_k	density of material k, g/cm^3 ($\equiv\langle\alpha_k\rho_0\rangle$)
τ_0	deviatiric stress
ϕ	particle shape factor, ($\phi = 1$ for spherical particle)
$\hat{\Phi}$	the gravitational potential
ψ_G	local gas flow dimensionless pressure drop, $\psi_G = (1/\rho_G g)(\Delta P/\Delta Z)$

Subscripts

j	the jth cell
X	x coordinate for the rectangular cell or bed
Z	axial coordinate along the length of bed
$\langle\ \rangle$	ensemble average (note: cross-sectional average in Eq. (15))
Min	minimization

capture of the gas velocity profile on a scale of a couple of particles not on the scale of the individual tortuous passages in the bed. We are not attempting to model the flow on a particle scale but to find the means for effectively computing the bed scale flow distribution provided the voidage distribution is known.

2. Non-parallel gas flow models

2.1. Vectorized Ergun equation model

This model is based on the assumption that a packed bed can be treated as a continuum. Therefore, it is assumed that the Ergun equation can be used in the differential, vector form as

$$-\nabla P = \mathbf{V}(f_1 + f_2 V). \tag{1}$$

The intent is to utilize the empirical Ergun equation, which is shown to hold well for overall pressure drop in macroscopic beds with unidirectional flow, for an infinitesimal length of the bed and apply it in the direction of flow. For an incompressible fluid, applying the curl operator ($\nabla\times$) to Eq. (1) yields Eq. (2), which is a vector equation containing the velocity vector $\mathbf{V}$ as the only dependent variable. The components of the velocity vector also have to satisfy the continuity Eq. (3):

$$-\nabla\times\mathbf{V} - \mathbf{V}\times\nabla[\ln(f_1 + f_2 V)] = 0, \tag{2}$$

$$\nabla\cdot\mathbf{V} = 0. \tag{3}$$

The solution for the velocity components can be obtained by solving Eqs. (2) and (3). A number of investigators (Stanek & Szekely, 1972,1973,1974; Szekely & Poveromo, 1975; Berning & Vortmeyer, 1987a) utilized this method to model two- and three-dimensional flow in packed beds.

2.2. Equations of motion model

In principle, the mass conservation (continuity equation) and momentum balance (Navier–Stokes equations) can be solved for the flowing phase provided the solid boundaries are precisely specified. Such a direct numerical simulation (DNS), however, is beyond reach at present for large industrial-scale packed beds (Joseph, 1998). By employing the effective viscosity as an adjusting factor, Ziolkowska and Ziolkowski (1993) and Bey and Eigenberger (1997) tried to develop a mathematical model for the interstitial velocity distribution based on the Navier–Stokes equations, but porosity was only considered as a function of radial position in such models. To take into account the complex fluid–particle interactions and the multi-dimensional variation of bed voidage in packed beds, a two-fluid (interpenetrating fluid) model provides a viable alternative (Johnson, Kashiwa & Vander Heyden, 1997). By ensemble averaging, the continuity and momentum equations for the flowing phase are formulated in a multi-dimensional form and the interphase interaction is described via appropriate drag correlation. The resulting equations can be solved via packaged computational fluid dynamics codes such as CFDLIB (Kashiwa, Padial, Rauenzahn & Vander Heyden, 1994) and FLUENT (Fluent 4.4, 1997), etc.

2.3. Discrete cell model (DCM)

This model is based on the concept that the bed may be represented by a number of interconnected discrete cells (Holub, 1990), with the bed porosity allowed to vary in two directions from cell to cell. The fluid flow is assumed to be governed by the minimum rate of total energy dissipation in the packed bed (*i.e. flow follows the path of the least resistance*). Ergun equation is assumed to be applicable to each cell. Therefore, the solution for velocity at each cell interface can be achieved by solving the non-linear multi-variable minimization problem.

Although the vectorized Ergun equation model (Stanek & Szekely, 1972) has provided a good description for non-parallel gas flow, it is still difficult to capture the non-uniformity of flow at the cell scale (few particles). It is also cumbersome to model the flow in beds with an internal random porosity profile because of the difficulties in arranging discrete porosity values to points in a continuum. Another difficulty of this model is the inability to set no-slip boundary conditions at the walls. The validity of the vectorized form of the Ergun equation was demonstrated only by comparison of the predicted exit velocity profile with experimental measurements. This kind of comparison is only reasonable for the parallel flow system that exhibits no effect of the packing support plate on the flow. Because of the above considerations, the discrete cell model was formulated as an alternative that may offer advantages in solving these problems. For example, the cell model is capable of capturing the non-parallel flow on a cell scale (few particles) due to the character of the cell model. The appropriate voidage can be assigned easily for each cell and the no-slip wall condition can be simulated by 'the extra cell method' (the detail discussion will be given later). It is assumed that the Ergun equation is applicable at the cell scale. This assumption is reasonable because the original Ergun equation was derived from the experimental measurements in small laboratory-scale packed beds (Ergun, 1952). The cell size has to be small compared to the bed scale (i.e., bed diameter), to obtain the desired resolution of the bed properties and flow distribution, but large compared to the particle scale (i.e., particle diameter) in order to apply the equation of Ergun (1952) to each discrete cell. The appropriate cell dimensions that satisfy these criteria were discussed by Vortmeyer and Winter (1984), who concluded that homogeneous models of packed-bed heat transfer failed in beds with a tube to particle diameter ratio less than three. While this conclusion was not reached for the exact situation considered here, a minimum linear dimension of about three particle diameters for each cell can be considered appropriate (Holub, 1990).

The second assumption of DCM is that the flow is governed by the minimum rate of total energy dissipation in the bed. The theoretical justification for this assumption has been provided only for linear systems, in which the fluxes and driving forces have a linear relationship, and rests on the principle of minimization of entropy production rate (Jaynes, 1980). For non-linear systems, examples can be constructed for which the 'principle of energy minimization' does not hold and, hence, that demonstrates that it is not a general 'principle' at all (Jaynes, 1980). Nevertheless, this energy minimization approach was reported to be valid for some classes of non-linear systems such as particle flow in circulating fluidized beds (Ishii, Nakajima & Horio, 1989; Li, Tung & Kwauk, 1988; Li, Reh & Kwauk, 1990). Hence, for any specific non-linear system one needs to conduct a detailed verification study before considering 'energy minimization' as the governing principle for flow distribution (Hyre & Glicksman, 1997). Regarding single-phase flow distribution in packed beds, it is necessary to revisit DCM by examining how well can this 'principle' be used to describe the flow. This can be done by comparing the results of the DCM to either accepted solutions of the ensemble-averaged momentum and mass conservation

equations or to reliable experimental data. Unfortunately, there is very few experimental data for the velocity profiles inside packed beds available in the literature due to the limitations on the non-intrusive velocity measuring techniques (McGreavy et al., 1986; Stephenson & Stewart, 1986; Peurrung et al., 1995). Thus, the objectives of this study are (i) to perform a series of numerical comparison studies of DCM predictions and CFD two-fluid model simulations, (ii) to compare the numerical results of DCM/CFD with the limited experimental data available in the literature, and finally, (iii) to reach a conclusion regarding the applicability of the 'minimization of energy dissipation' concept in modeling single-phase flow distribution in packed beds.

Another motivation for this study is the fact that the concept of minimization of the rate of energy dissipation was never tested against the solution of the full set of equations of motion for a non-parallel flow system. Now, we provide such a test for flow distribution in packed beds. The results should generate a better appreciation of what the concept of minimization of the total energy dissipation rate can and cannot do.

3. Discrete cell model (DCM)

The discrete cell model based on the minimization of energy dissipation rate presented and discussed here is adapted from the concept originally proposed by Holub (1990). Although a 2D-model bed is considered here, its extension to 3D axi-symmetric cases is readily accomplished. The 2D rectangular model bed shown in Fig. 1 is divided into a number of cells, each of which is assumed to have uniform porosity within itself and have two fluid velocity components (V_z and V_x) at each cell interface.

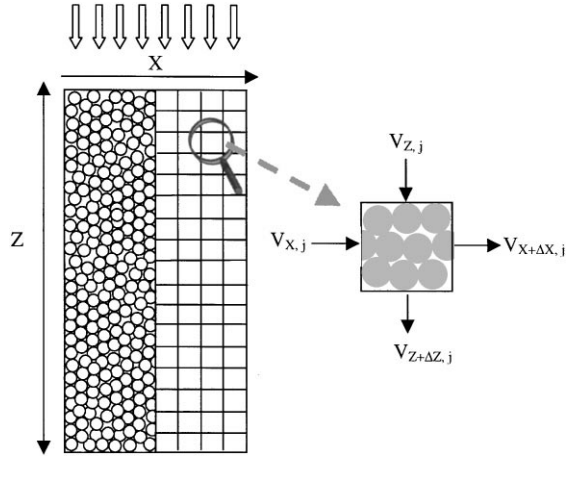

Fig. 1. Model packed bed ('*2D' rectangular packed bed as example*) and velocity at each interface of cell *j*. (Note that $S_{x,j}$ equals to $S_{X+\Delta X,j}$ in the '2D' rectangular packed bed).

The porosity can vary from cell to cell. The rate of energy dissipation for each cell can then be derived from the macroscopic mechanical energy balance and results in Eq. (4) in X–Z coordinates for either two-dimensional rectangular (2D) or three-dimensional axi-symmetric cylindrical (3D) situation. The differences in Eq. (4) for 2D rectangular and 3D axial symmetric cylindrical bed are the expressions for the interface areas (S_i) and the cell volumes ($V_{c,j}$). Details of the derivation of Eq. (4) are given in the appendix.

$$\begin{aligned} E_{V,j} = \frac{1}{2}\Bigg\{ & \frac{\rho}{\varepsilon_j^2}(V_X^3 S_X - V_{X+\Delta X}^3 S_{X+\Delta X})_j \\ & + \frac{\rho}{\varepsilon_j^2}(V_Z^3 S_Z - V_{Z+\Delta Z}^3 S_{Z+\Delta Z})_j \\ & + (f_{1,j} V_{X,j}^2 + f_{2,j} V_{X,j}^2 |V_{X,j}| + f_{1,j} V_{X+\Delta X,j}^2 \\ & + f_{2,j} V_{X+\Delta X}^2 |V_{X+\Delta X,j}|) V_{C,j} \\ & + (f_{1,j} V_{Z,j}^2 + f_{2,j} V_{Z,j}^2 |V_{Z,j}| + f_{1,j} V_{Z+\Delta Z,j}^2 \\ & + f_{2,j} V_{Z+\Delta Z,j}^2 |V_{Z+\Delta Z,j}|) V_{C,j} \Bigg\}. \end{aligned} \tag{4}$$

In Eq. (4) $f_{1,j}$ and $f_{2,j}$ are Ergun coefficients (Ergun, 1952) defined as follows:

$$f_{1,j} = \frac{150\mu(1-\varepsilon_j)^2}{(\phi d_P)^2 \varepsilon_j^3}, \tag{5}$$

$$f_{2,j} = \frac{1.75\rho(1-\varepsilon_j)}{(\phi d_P)\varepsilon_j^3}. \tag{6}$$

In this study, we use the 'universal values' ($E_1 = 150, E_2 = 1.75$) to calculate $f_{1,f}$ and $f_{2,f}$ as done by most other investigators (Vortmeyer & Schuster, 1983; Stanek, 1994; Bey & Eigenberger, 1997). Although E_1 and E_2 values can vary from macroscopic bed to bed due different structures of the packing in the bed (MacDonald, El-Sayed, Mow & Dullien, 1979), this effect can be accounted for by the assignment of a non-uniform porosity distribution instead of using the average porosity value for the bed.

The complete model for determining the gas flow distribution in the bed requires the minimization of the rate of total energy dissipated with the cell velocities as variables. It is a non-linear, multivariable minimization problem (Eq. (7)) subject to mass balance constraint for each cell (Eq. (8), based on constant fluid density assumption), and constraints for bed boundaries. The setting of cell boundary conditions reflect the internal structural non-uniformities and operating conditions. In other words, this model can predict the gas flow distributions in packed beds with various operating conditions (i.e. side gas feed) and with different internal structural

non-uniformities:

$$\text{Min}\,[E_{v,\text{bed}}] = \text{Min}\left[\sum_{j=1}^{N} E_{v,j}\right], \tag{7}$$

$$(V_X S_X - V_{X+\Delta X} S_{X+\Delta X})_j + (V_Z S_Z - V_{Z+\Delta Z} S_{Z+\Delta Z})_j = 0. \tag{8}$$

The subroutine DN0ONF from the International Mathematical Statistics Library (IMSL) was used to solve this constrained non-linear minimization problem and obtain the fluid velocity components V_x and V_z for each cell in the bed.

4. CFDLIB formulations

CFDLIB, a library of multi-phase flow codes developed by Los Alamos National Laboratory (Kashiwa et al., 1994), has been used to obtain the results for comparison with the DCM predictions. The solution algorithm is a cell-centered finite-volume method applied to the time-dependent conservation equations (Kashiwa et al., 1994). The governing equations that serve as the basis for the CFDLIB codes are:

Equation of continuity:

$$\frac{\partial \rho_k}{\partial t} + \nabla\cdot \rho_k u_k = \langle \rho_k \dot{\alpha}_k \rangle. \tag{9}$$

The terms on the left-hand side of Eq. (9) constitute the rate of change in mass of phase k at a given point, and the term on the right-hand side is the source term due to conversion of mass from one phase to the other. In present study this term is equal to zero since no phase change, reaction or mass transfer is considered in this cold flow modeling.

Equation of momentum:

$$\begin{aligned}
&\frac{\partial \rho_k \mathbf{u}_k}{\partial t} + \nabla\cdot \rho_k \mathbf{u}_k \mathbf{u}_k \\
&\quad = (\text{rate of change in } k\text{th phase momentum}) \\
&\qquad + \langle \rho_0 \mathbf{u}_0 \dot{\alpha}_k \rangle \\
&\qquad (\text{net mass exchange source of } k) \\
&\qquad - \nabla\cdot \langle \alpha_k \rho_0 \mathbf{u}_k' \mathbf{u}_k' \rangle \\
&\qquad (\text{multiphase Reynolds stress}) \\
&\qquad - \theta_k \nabla p \\
&\qquad (\text{acceleration by the equilibration pressure}) \\
&\qquad + \nabla\cdot \langle \alpha_k \bar{\bar{\tau}}_0 \rangle \\
&\qquad (\text{acceleration due to average material stress}) \\
&\qquad - \nabla\theta_k (p_0^k - p) \\
&\qquad (\text{acceleration by non-equilibrium pressure}) \\
&\qquad + \rho_k \mathbf{g} \\
&\qquad (\text{acceleration by body force}) \\
&\qquad + \langle [(p_0 - p)\boldsymbol{I} - \bar{\bar{\tau}}_0] \cdot \nabla \alpha_k \rangle \\
&\qquad (\text{momentum exchange terms}).
\end{aligned} \tag{10}$$

This set of equations is exact with no approximations other than the ensemble averaging used in the two-fluid model approaches (Ishii, 1975). The special case of one fixed phase (the catalyst bed) has been incorporated into the code for single-phase flow simulation (Kumar, 1995). In Eqs. (9) and (10), the mass source term is considered as zero due to the absence of reaction or interphase transport. The important term is the interphase momentum exchange term, which is modeled by a choice of the appropriate drag closure. Contribution of Reynolds stress can be ignored for most cases for flow through packed beds. The detail discussions of this term will be given later. One of the advantages of CFDLIB is that there are options for specifying user-defined drag forms based on each combination of the phases under consideration. In this study, the same drag force formulation as used in the Ergun equation is employed for both CFDLIB (exchange term in Eq. (10)) and DCM simulations. This is a realistic drag correlation at the cell scale as mentioned earlier, and it has been used by many other investigators point-wise in packed beds (Vortmeyer & Schuster, 1983; Stanek, 1994; Song, Yin, Nandakumar & Chuang, 1998). CFDLIB code also allows the choice of velocity and pressure boundary conditions for inflow, outflow and free slip or no slip at the wall boundaries. To keep the consistency with the discrete cell approach used in DCM, the spatial discretization of the model bed is the same in both methods as the cell scale (few particles).

5. Modeling results and discussion

5.1. Model packed bed

The model bed used for this numerical study is a two-dimensional packed bed with a predetermined pseudo-random porosity distribution as shown in Fig. 2. The average porosity of this bed is 0.415, and was obtained experimentally in an identical '2D' rectangular bed with spherical particles of 3 mm diameter. The porosity profiles in the internal region of the bed were generated by a computer program under certain constraints (range: 0.360–0.440; mean: 0.406), which is fairly close to that obtained by dumping spheres into beds (Tory, Church, Tam & Ratner, 1973). A relatively higher porosity of 0.44 was assigned to the wall and the support plate regions based on the typical porosity profiles reported in the

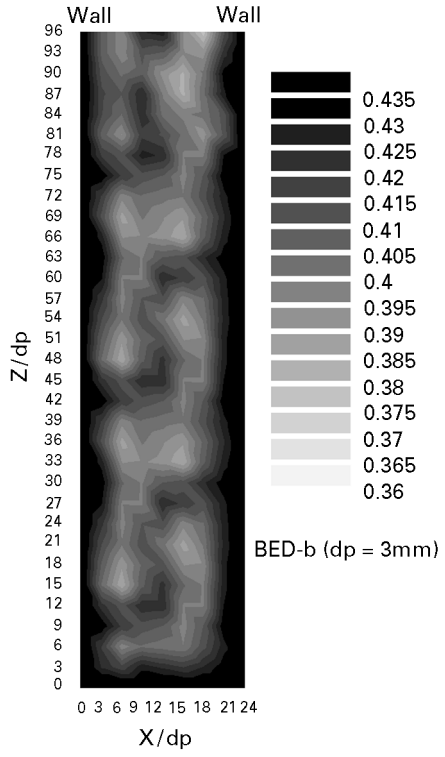

Fig. 2. Porosity distribution of model bed (32 cells × 8 cells): Total average porosity: 0.415; internal region: 0.36–0.44 (random distribution); wall region: 0.44; Two limits (0.36 and 0.44) correspond to the dense packing and loose packing porosity. When two obstacle plates are placed in this system, one is located at Z/d_p of 66 (at the left side), another is at Z/d_p of 30 (at the right side). The width of the obstacle plate (i.e. the length that it protrudes into the bed) is half of the width of bed (4 cells).

literature (Benenati & Brosilow, 1962; Haughey & Beveridge, 1969). The dimensions of the model bed and of the cells as well as physical properties of the fluid (gas) are given in the notation section. The bed walls are considered to be impermeable in the normal direction (X direction) and allow free-slip in the parallel direction (Z direction). In order to implement the no-slip boundary conditions in DCM, the 'ghost cell' method could be used in which an extra column of cells outside the bed can be set and assigned an extremely low porosity (i.e. less than 0.01). Thus, the effect of bed wall and no slip boundary condition on gas flow could in principle be considered in this way. It should be noted that the use of DCM is not limited to spherical particles. It can be applied to any shape of particles by taking into account the particle shape factor, ϕ, in Eqs. (5) and (6).

5.2. Analysis of energy dissipation equation

As shown in Eq. (4), there are three terms contributing to the total energy dissipation rate per unit cell: inertial loss (T_i), viscous loss (T_v), and kinetic energy loss (T_k).

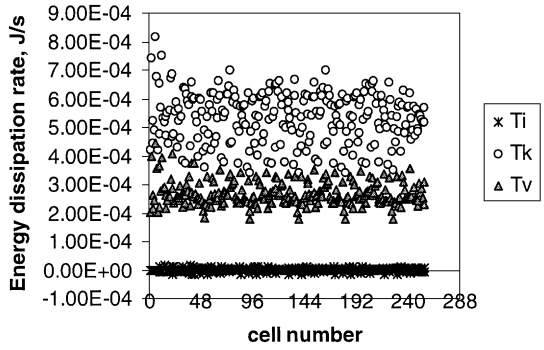

Fig. 3. Contribution of each energy dissipation rate term at each cell to the total energy dissipation rate. $V_0 = 0.5$ m/s (gas flow without internal obstacles); $Re' = 28.5$; $\sum_{n=1}^{256} T_i = -6.85 \times 10^{-5}$ J/s; $\sum_{n=1}^{256} T_k = 1.37 \times 10^{-1}$ J/s; $\sum_{n=1}^{256} T_v = 6.87 \times 10^{-2}$ J/s; $\sum_{n=1}^{256}(T_i + T_k + T_v) = 2.056 \times 10^{-1}$ J/s. (The cell number is counted from the top left of the bed in the X direction.).

The contribution of the gravitational potential term has been ignored for gas flow due to the low density of the fluid (this term is accounted for when liquid flow is considered). The expressions for these three terms in cell j are

$$T_{i,j} = \frac{\rho}{2\varepsilon_j^2}(V_X^3 S_X - V_{X+\Delta X}^3 S_{X+\Delta X})_j + \frac{\rho}{2\varepsilon_j^2}(V_Z^3 S_Z - V_{Z+\Delta Z}^3 S_{Z+\Delta Z})_j, \quad (12)$$

$$T_{k,j} = (f_{2,j} V_{X,j}^2 |V_{X,j}| + f_{2,j} V_{X+\Delta X}^2 |V_{X+\Delta X,j}| + f_{2,j} V_{Z,j}^2 |V_{Z,j}| + f_{2,j} V_{Z+\Delta Z}^2 |V_{Z+\Delta Z,j}|) V_{C,j}, \quad (13)$$

$$T_{V,j} = (f_{1,j} V_{X,j}^2 + f_{1,j} V_{X+\Delta X,j}^2 + f_{1,j} V_{Z,j}^2 + f_{1,j} V_{Z+\Delta Z,j}^2) V_{C,j}. \quad (14)$$

As derived in the appendix, the pressure drop term is substituted by $T_{k,j}$ and $T_{v,j}$ to eliminate the pressure term (see Eqs. (A.6) and (A.8)). This is rigorously true only when inertial terms are zero and no source terms due to interphase transport are present in the continuity equation. Hence, we still consider the inertial terms in Eq. (4) so as to account for flow with abruptly changing direction. The significance of this term is examined for a low-density gas flow (where it is expected to be negligible), a high-density liquid flow, and gas flow with internal obstacles (where it can approach in magnitudes the other terms). For a non-parallel gas flow test case (Reynolds number, Re' of 28.5), Fig. 3 shows the contribution of each energy dissipation rate term to the total energy dissipation rate. One should note that the Reynolds number (Re') in this paper is defined on the basis of the input superficial velocity V_0 and the inverse of the specific

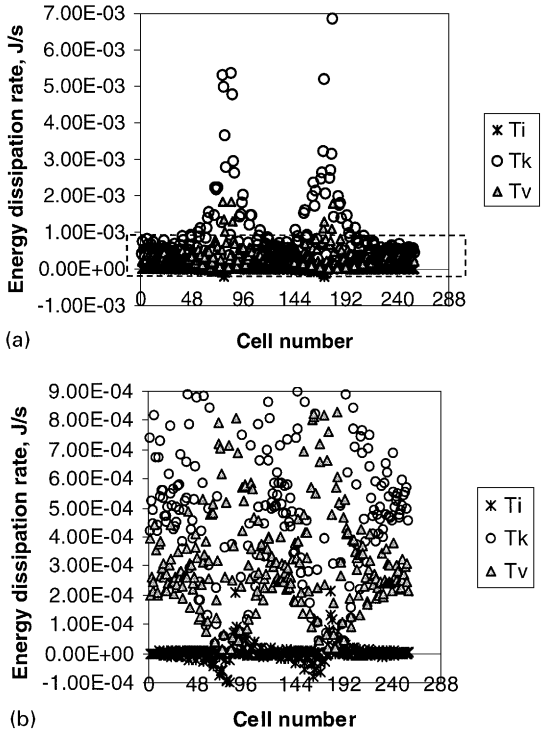

Fig. 4. (a) Contribution of each energy dissipation rate term at each cell to the total energy dissipation rate. $V_0 = 0.5$ m/s (gas flow with two internal obstacles at $Z/d_p = 30, 66$); $Re' = 28.5$; $\sum_{n=1}^{256} T_i = -1.22 \times 10^{-4}$ J/s; $\sum_{n=1}^{256} T_k = 2.15 \times 10^{-1}$ J/s; $\sum_{n=1}^{256} T_v = 0.905 \times 10^{-1}$ J/s; $\sum_{n=1}^{256}(T_i + T_k + T_v) = 3.06 \times 10^{-1}$ J/s. (The dashed line region will be re-illutstrated in Fig. 4b). (b) Contribution of each energy dissipation rate term at each cell to the total energy dissipation rate. $V_0 = 0.5$ m/s (gas flow with two internal obstacles at $Z/d_p = 30, 66$); $Re' = 28.5$; $E_{\text{bed}} = \sum_{n=1}^{256}(T_i + T_k + T_v) = 3.06 \times 10^{-1}$ J/s.

surface of particles as the length scale (see notation) which is the same as that in Stanek (1994). It can be converted to the particle Reynolds number (Re_p) used in some studies by multiplying it with a factor of $6(1 - \varepsilon_B)$ (~ 3.51 in this study). It was found that when no internal obstacles are present and the flow is nearly parallel, the inertial term (T_i) is negligible compared to the other two terms (T_k and T_v). The viscous term (T_v) is about one-third of the total energy dissipation rate, and the kinetic term (T_k) is two-thirds of the total energy dissipation rate. However, when two obstacle plates are placed in the above packed bed to create significantly non-parallel flow (see Fig. 2), their effect on the total energy dissipation rate per unit cell is significant as shown in Fig. 4a. The total energy dissipation rate is almost 50% higher compared to the one without the internal obstacles. The inertial term (T_i) is still negligible compared to the other two terms (T_k and T_v) except in the very proximity of the obstacles as shown in Fig. 4b. The values of T_k and T_v are scattered, but of the same order. Higher values of T_k are observed at the obstacle regions as shown in Fig. 4b. It is clear that internal obstacles make the gas

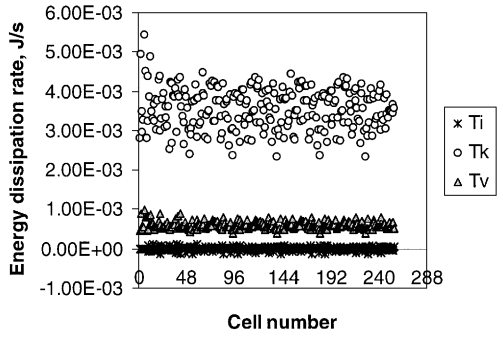

Fig. 5. Contribution of each energy dissipation rate term at each cell to the total energy dissipation rate. $V_0 = 0.1$ m/s (liquid flow without internal obstacles); $Re' = 47.5$; $\sum_{n=1}^{256} T_i = -5.79 \times 10^{-4}$ J/s; $\sum_{n=1}^{256} T_k = 9.1 \times 10^{-1}$ J/s; $\sum_{n=1}^{256} T_v = 1.53 \times 10^{-1}$ J/s; $\sum_{n=1}^{256}(T_i + T_k + T_v) = 10.624 \times 10^{-1}$ J/s.

flow more non-uniform. The possibility of dominant inertial term was examined for a case with high-density fluid by simulating a saturated liquid flow case. Here, the kinetic term (T_k) is seen to be dominant in the energy dissipation rate per unit cell at liquid superficial velocity, U_0 of 0.1 m/s ($Re' = 47.5$). The inertial term (T_i) is not significant even in this case as shown in Fig. 5. It can be concluded that the inertial term is not important except in the obstacle region which is in agreement with the simulations reported in the literature (Choudhary, Propster & Szekely, 1976). This also justifies the substitution of the pressure drop by the Ergun equation terms (T_k and T_v) and elimination of the pressure term from the equation completely. In general, however, it is still advisable to include the inertial term in the formulation of total energy dissipation per unit cell to account for those highly non-uniform flow situations in which the *inertial terms* could be important in affecting the nature of flow (Choudhary et al., 1976).

Regarding the contribution of the Reynolds stress term to the cell-scale velocity distribution in packed beds, we performed CFDLIB simulations of liquid up-flow at a high particle Reynolds number (Re_p) of 600 ($V_1 = 0.2$ m/s) with and without turning on a simple turbulence model based on the mixing-length concept (using particle diameter as a sample of mixing length). The relative differences in simulated liquid velocity profiles in the two cases are negligible (less than 0.1%). This implies that the contribution of the Reynolds stress term to the cell scale (i.e. 0.9 cm = 3 particles) flow distribution in packed beds is negligible. However, such term may become important if one attempts to model the local particle scale (less than one particle diameter) flow field. As a matter of fact, the transition between laminar and turbulent flow regime occurs in a certain particle Reynolds number range (Re_p), which may vary with particle diameter. For instance, the critical Reynolds number range of 150–300 was reported by Jolls and

Hanratty (1969) for particles of 1.27 cm in diameter while Latifi et al. (1989) reported the range of 110–370 for 0.5 cm diameter glass beads. This data were locally measured by using micro-electrodes with a diameter of 25 μm (Latifi, Midoux & Storck, 1989) and reflects the flow behavior in the interstitial space in packed beds. The recent fine-mesh CFD simulation by Nijemeisland, Logtenberg & Dixon (1998) did find the stronger turbulent eddies in the gaps in between the spheres at higher Reynolds number flow conditions.

In the development of the DCM, we made use of the fact that pressure at the orthogonal directions P_{cx} and P_{cz} has the same magnitude at the center of the cell. We could then eliminate the central pressure term from the expression for the energy dissipation rate per unit cell (Eq. (A.6)) by using the mass balance for each cell. In order to ensure that this formulation is consistent, we have back calculated the central pressure (P_{cx} and P_{cz}) based on the two-dimensional velocity solution (V_z and V_x) and verified that they do have the same values at the center of each cell as required, although the pressure drop in the X and Z directions may have different values.

Due to the non-linearity of the equations (cubic in velocity), another important consideration is the uniqueness of the velocity obtained by solution of the minimization problem solved in DCM. To examine this, different starting guess values varying over two orders of magnitude were used for a test case (input superficial velocity, $V_0 = 0.1$ m/s). For this case, starting guessed values anywhere between -1.0 and $+1.0$ m/s converged to a unique solution for velocity based on the minimum total energy dissipation rate.

With regard to the computational efficiency of DCM, for the cases considered in this study (total cell number: $264 = 256_{\text{packing zone}} + 8_{\text{supporting plate}}$; the corresponding number of variables in the optimization is 569), the computation time is comparable with that required to execute the CFDLIB code with identical discretization. It is noted, however, that simulation of a case with a larger number of cells would require a more effective non-linear multi-variable optimization algorithm to get better computational efficiency.

5.3. Comparison of DCM and CFDLIB

The verification of DCM predictions can be obtained by comparing them with the fluid dynamic model solutions (CFDLIB) under identical physical and operating conditions. For the simplified case of 'parallel flow', Stanek (1994) argued that the solutions for velocity obtained by the two methods, *differential vectorial Ergun equation model* (based on momentum equation) and *minimum rate of energy dissipation method* are identical in both limiting ranges of the Reynolds number (fast flow, i.e. $Re' \geqslant 150$, and slow flows, i.e. $Re' \leqslant 1.5$). This conclusion was reached by comparing the analytical solutions of the two methods. In the transition region ($1.5 < Re' < 150$), however, the minimum rate of energy dissipation method yielded smaller velocities (Stanek & Szekely, 1974; Stanek, 1994) than the vectorized Ergun equation. As mentioned earlier, the rate of energy dissipation term due to *inertia* was ignored in the differential vectorized Ergun equation model (Kitaev et al., 1975). For the case of two-dimensional 'non-parallel flow', which is of interest in this study, the conclusions regarding the applicability of the minimum rate of energy dissipation concept in providing a comparable solution for the gas velocity at cell scale need to be reconsidered. However, analytical solution of the fluid dynamic equations for 'non-parallel flow' are unavailable; therefore, the numerical results from computational fluid dynamic solution (CFDLIB) are used for verification of the DCM simulation results. In order to compare them effectively, the same operating conditions and the same structure of the bed are used in the simulations. To cover a wide range of Reynolds numbers, three sets of superficial gas velocity of 0.1, 0.5, 3.0 m/s are chosen. The corresponding Reynolds numbers (Re') are 5.7, 28.5, and 170.9, respectively. Three sets of results at different Reynolds number are shown in Figs. 6–8 at different axial positions ($Z/d_p = 4.5$, 19.5, 34.5, 49.5, 64.5, 79.5 from the top of bed).

Following the work of Stephenson and Stewart (1986), and Cheng and Yuan (1997), we use the (relative) local superficial velocity defined as

$$(\textit{Relative})\ \textit{local superficial velocity} = \frac{U_j \varepsilon_j}{\langle U_j \varepsilon_j \rangle} = \frac{V_j}{V_0}, \quad (15)$$

i.e. the local interstitial velocity times the local porosity (for single-phase flow) divided by the cross-sectionally averaged superficial velocity as given in Eq. (15). It is found that the simulated local (i.e. cell scale) gas superficial velocity profiles by both DCM and CFD at each given axial position track the porosity profile very well. Higher local porosity corresponds to higher local velocity. The difference in prediction between DCM and CFD simulation was found to be less than 10% over the whole range of Reynolds numbers ($Re' = 5$–171) as shown in Figs. 9a and b. It is also shown that the relative local velocities vary in the range of 0.8–1.2 for the given system with a porosity variation of a cell scale (i.e. 0.9 cm). This means that the velocity profiles from DCM and CFDLIB compare well at three different Reynolds numbers. Reasonable comparisons of these two modeling approaches are achieved even at high Re' number ($Re' = 170.9$ at $V_0 = 3.0$ m/s). This implies that DCM based on the minimum rate of energy dissipated can provide us with gas velocity predictions comparable to those obtained by CFD, which rests on ensemble-averaged mass and momentum conservation equations.

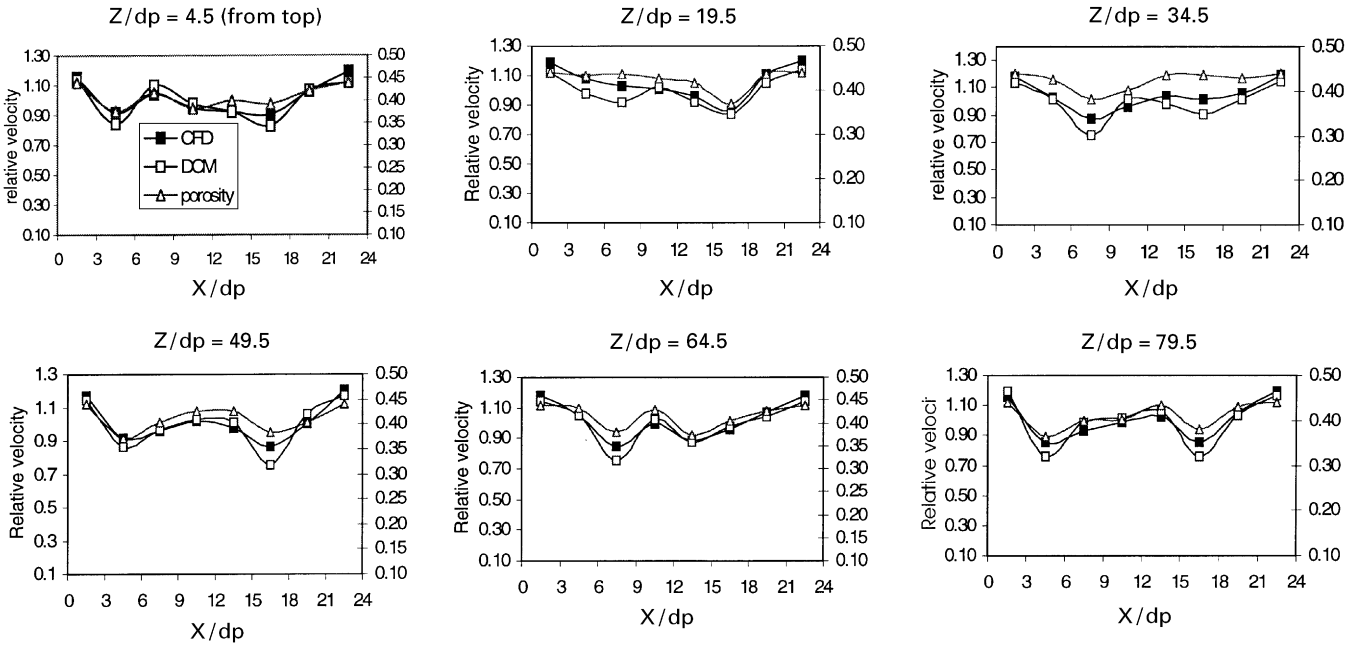

Fig. 6. Comparison of CFD simulations and DCM predictions at a superficial velocity of 0.1 m/s at different axial positions (Z/d_p) ($Re' = 5.7$). Left axis is the relative cell superficial velocity; right axis is the cell porosity.

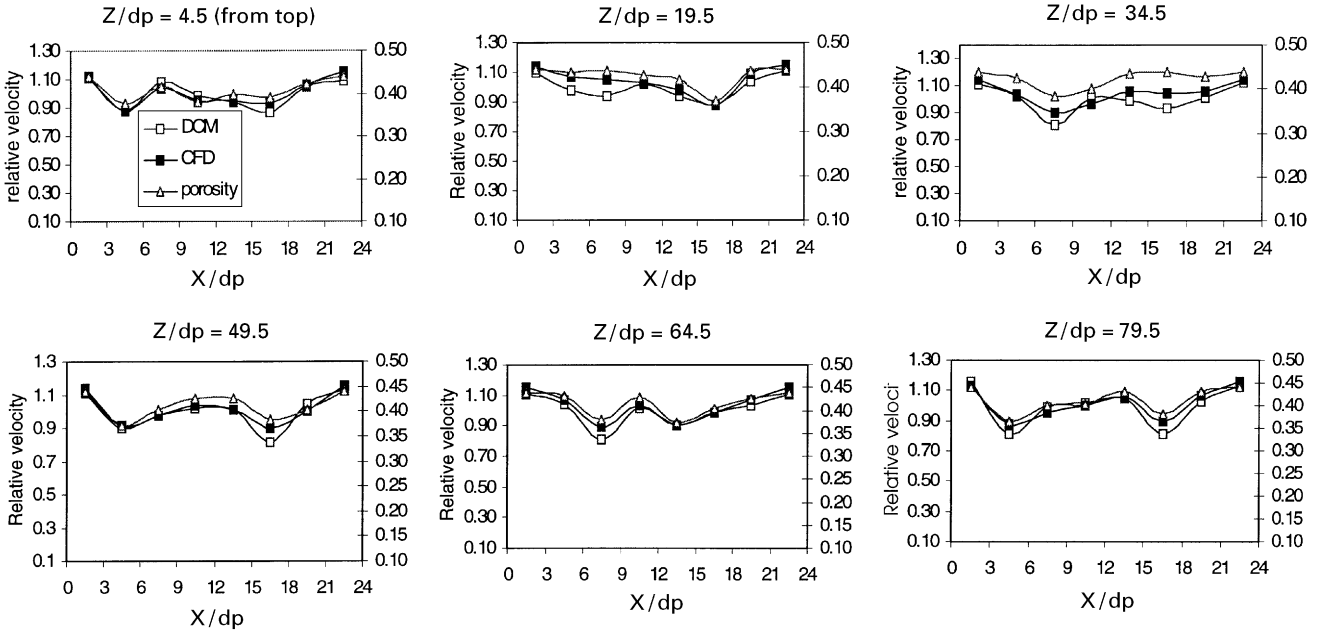

Fig. 7. Comparison of CFD simulations and DCM predictions at a superficial velocity of 0.5 m/s at different axial positions (Z/d_p) ($Re' = 28.5$).

To examine the effect of fluid density and gravity, the calculations by both methods were repeated for liquid flow through a liquid-saturated bed. In practice, this would be the case of liquid up-flow through the packed bed. It should be noted that the gravity term has now to be accounted for (see Eq. (A.2)) because Eq. (A.3) is not satisfied for liquid flow. The difference in prediction of V_z (velocity component in the Z direction) between DCM and CFD simulation was found to be less than 10% for the liquid superficial velocity of 0.1 m/s ($Re' = 47.5$). DCM yields a 1–2% lower prediction of V_z than CFD as shown in Fig. 10a. Correspondingly, a lower prediction

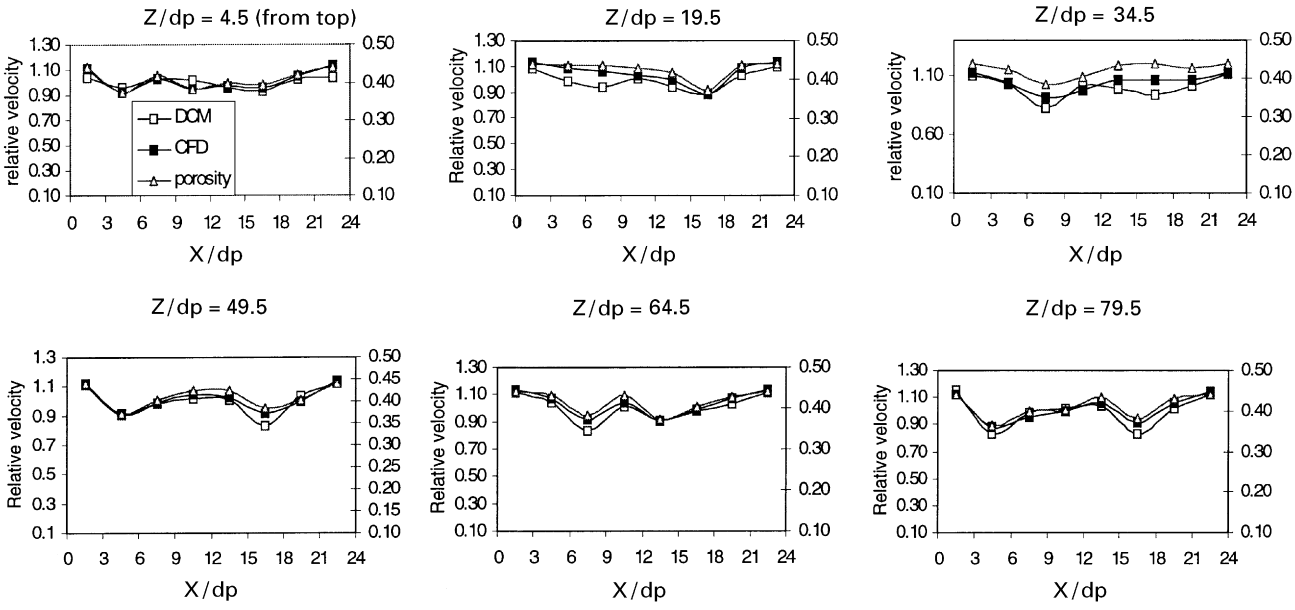

Fig. 8. Comparison of CFD simulations and DCM predictions at a superficial velocity of 3.0 m/s at different axial positions (Z/d_p) ($Re' = 171$).

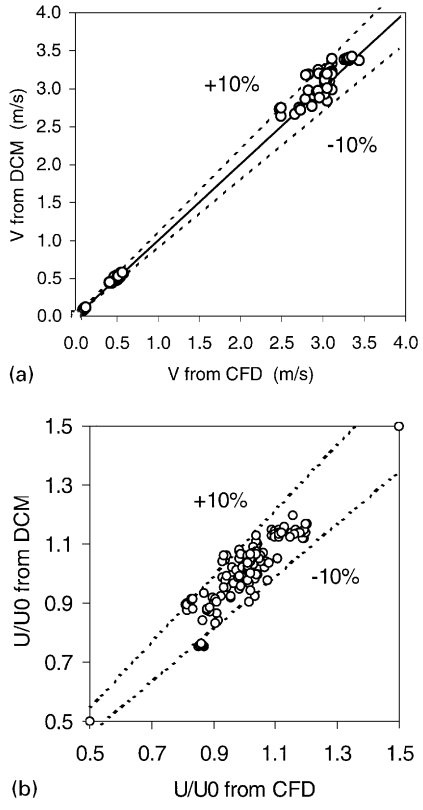

Fig. 9. Comparison between CFD and DCM predictions for gas flow in the Reynolds number (Re') range of 5–171: (a) superficial velocity (V_j); (b) relative interstitial velocity (U_j/U_0); $U_0 = V_0/\varepsilon_B$.

of V_x (velocity component in the X direction) was found in CFD as shown in Fig. 10b. This implies that in a liquid–solid system the prediction by DCM is a little bit more sensitive to the bed structure such as porosity distribution than CFD. From a practical point of view, this feature of DCM prediction for liquid flow does not diminish its appeal as the method of providing a reasonable solution. This also implies that DCM is applicable for modeling of the high-pressure gas–solid systems in which the density of the gas is high.

5.4. Comparison of DCM/CFDLIB and experiment data

As discussed earlier, most experimental studies in the literature reported the velocity profiles at the bed exit (Morales et al., 1951; Szekely & Poveromo, 1975; Bey & Eigenberger, 1997). They could provide the data only for validating the model prediction for the velocity profile downstream of the bed (see Bey & Eigenberger, 1997; Subagyo et al., 1998). For non-parallel flow system of interest in this study, the exit velocity profile cannot represent the flow behavior inside the bed (Lerou & Froment, 1977; McGreavy et al., 1986). Hence, experimental data inside packed beds is needed to perform the proper comparison of DCM/CFDLIB predictions and experimental results. The liquid velocity profile inside the bed of Stephenson and Stewart (1986) is useful for such a comparison because both porosity and velocity data were reported in their paper. However, the data are still inadequate for a very rigorous comparison of the numerical simulation and experiments since only one set of data was reported, and this was an ensemble-averaged result based on a large number of 'cell' measurements. Nevertheless, for lack of better data, this information has been used by others for model validation (Cheng & Yuan, 1997; Subagyo et al., 1998). The single-phase flow distribution data of McGreavy et al. (1986) inside the packed bed is only good for a qualitative test of numerical

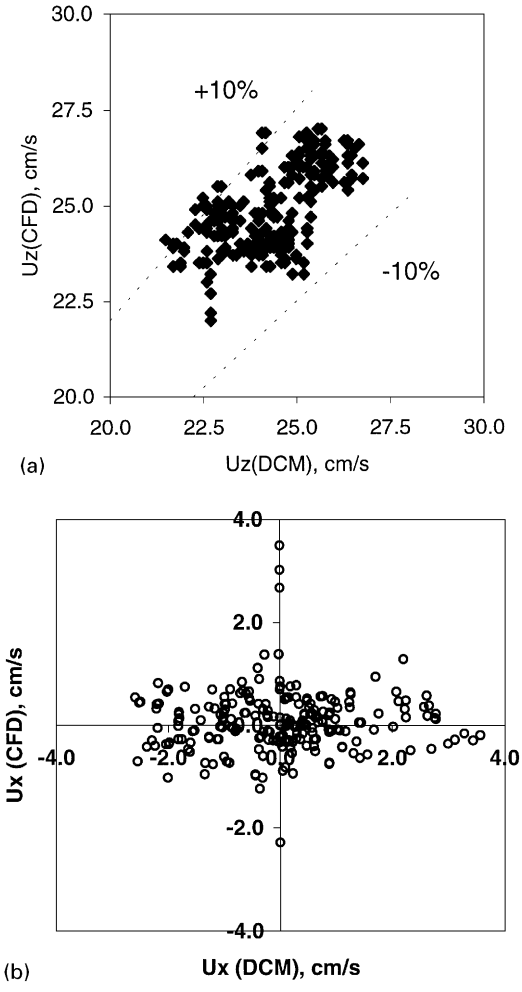

Fig. 10. (a) Comparison of predicted interstitial velocity component in the Z direction (U_z) by two methods in liquid up-flow system: liquid superficial velocity $V_0 = 0.1$ m/s ($Re' = 47.5$). (b) Comparison of predicted interstitial velocity component in the X direction (U_X) by two methods in liquid up-flow system: inlet liquid superficial velocity $V_0 = 0.1$ m/s.

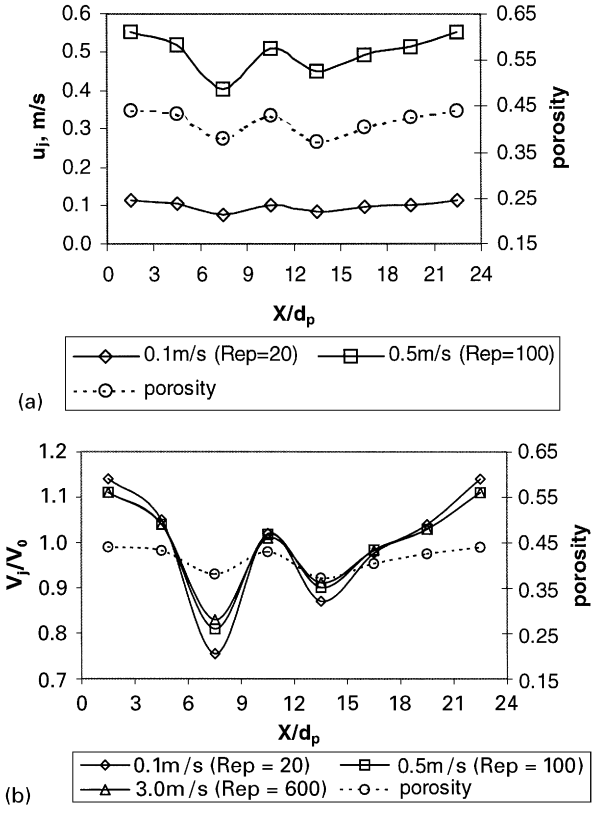

Fig. 11. (a) Influence of gas feed superficial velocity on DCM predicted cell interstitial velocity profiles. (b) Effect of particle Reynolds number (Re_p) on the calculated relative cell superficial velocity profile inside a bed.

simulations because the corresponding porosity data was not reported (see Fig. 7 in McGreavy et al., 1986).

Figs. 11a and b display the DCM results indicating the effect of fluid feed velocity (or particle Reynolds number, Re_p) on the velocity profile inside the bed, which are qualitatively comparable with the experimental data of McGreavy et al. (1986) (see Figs. 7 and 8 in that paper). The high velocity zones match the high voidage regions, as would be expected, and as the flow increases the magnitude of these peaks become more pronounced. Fig. 11b is also comparable with the recent independent modeling result of Subagyo et al. (1998) (see Fig. 9 in their paper). The same conclusions are evident as reported by Subagyo et al. (1998) that for Re_p less than 500, the velocity profile is dependent on the particle Reynolds number. On the other hand, the effect of the Reynolds number on the velocity profile is no longer significant for Re_p higher than 500.

The quantitative comparison of our numerical simulations (CFDLIB) has been carried out with the data of Stephenson and Stewart (1986) in which the velocity and voidage data were obtained by using optical measurements for Reynolds numbers of 5 and 80 in beds with D/d_p ratio of 10.7. Velocity was measured inside a bed of cylindrical particles ($d_v = 0.703$ cm) with liquid flows of very different physical properties (ρ_L;μ_L). To simulate the experimental bed, a 2D axi-symmetric bed in cylindrical coordinates ($r - Z$) is chosen in CFDLIB simulation. The radial spatial discretization ($N_c = 20$) is the same as that used as the viewing zone for collecting each experimental data point (i.e. a space interval of $\Delta = 0.05R$). In addition, no-slip wall boundary and liquid gravity effect are accounted for in the simulations. The experimentally reported radial porosity profile is used in CFDLIB simulation. Fig. 12 shows the comparison of CFDLIB simulated relative superficial velocity profile (V_z) and the measured data at Re_p numbers of 5 and 80. Good agreement is achieved. This implies that even for a cell size less than a particle diameter, CFDLIB code can still provide a reasonable prediction of the velocity profile. The same

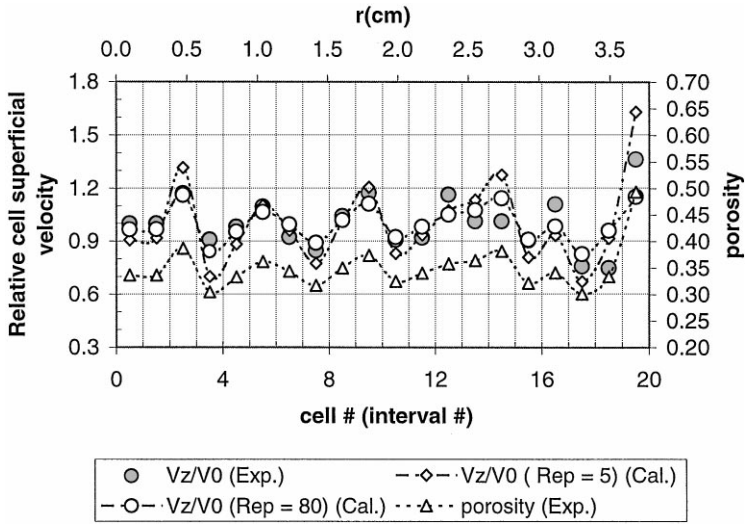

Fig. 12. Relative liquid cell superficial velocity comparison of experimental measured data of Stephenson and Stewart (1986) and CFDLIB simulated results in a packed bed with $D/d_V = 10.7$ and $d_V = 0.7035$ cm (cylindrical particles). Physical properties of liquid: Liquid -B for condition at a Re_p of 5, $\rho = 1.125$ g/cm^3; $\mu = 0.474$ g cm/s. Liquid -C for condition at Re_p of 80, $\rho = 1.027$ g/cm^3; $\mu = 0.114$ g cm/s.

agreement between DCM and the experimental data of Stephenson and Stewart (1986) is expected since DCM and CFDLIB have always provided results with 10% of each other as discussed in Section 5.3. One should note that the above comparison of CFDLIB and the experimental data still rests on the one-dimensional porosity variation (e.g. radial direction). Because of the lack of the two-dimensional measured porosity distribution and velocity distribution data reported in the paper by Stephenson and Stewart (1986), it is impossible to conduct the full comparison of simulated two-dimensional velocity field by DCM/CFDLIB with two-dimensional experimental data of flow distribution at the cell scale.

5.5. Case studies by DCM

Since the validity and accuracy of DCM are established in the previous sections, DCM can be used in engineering applications as demonstrated in the case studies considered here. Because of the discrete nature of DCM, boundary conditions can be easily set. The local variation of porosity can also be accommodated readily. It is possible to use DCM to model two- or three-dimensional non-parallel flow fields. Two cases are considered to demonstrate these claims: (i) a bed with pseudo-random porosity distribution and internal obstacles was considered; and (ii) two types of gas flow inlets (top and side gas inlets) are examined using the DCM method. Velocity vector plots and pressure and dimensionless pressure drop contour plots are shown in Figs. 13a, b, 14a, b, respectively. Figs. 13a and b illustrate the dependency of the gas velocity field on the internal structure non-uniformities inside the beds (i.e. two internal obstacle plates) and the effect of irregular gas feed (i.e. side gas input) as well as of the pseudo-random porosity distribution. No vortices appear in the vicinity of the obstacle plates or at least they are not larger than the cell size. The predicted results for velocity are almost symmetric with respect to the obstacle plate, which is in good agreement with the Berning and Vortmeyer (1987a,b) findings obtained by the *vectorized Ergun equation* method. The effect of side gas feed ('point source') was evident not only in the entrance region, but also in downflow regions as shown in Fig. 13b at given operating conditions, although no effect could be detected at the exit. Therefore, it is difficult to draw the proper conclusion about the effect of side gas feeding on the flow field based only on the exit velocity measurements (Szekely & Poveromo, 1975). It is expected, however, that the effect of side feed will depend on the magnitude of the side feed gas velocity. The full pressure field in the packed bed with two internal obstacles is shown in Fig. 14a. Higher local pressure drop occurs at the regions around internal obstacles. This is not surprising due to the higher velocity and higher flow resistance in these regions. Fig. 14b shows the dimensionless local pressure drop ($\psi_G = (1/\rho_G g)(\Delta P/\Delta Z)$) in the case of the side gas feed. Higher values of ψ_G are evident in the entry and obstacle regions. In contrast, lower values of ψ_G are apparent in the corner regions.

6. Remarks

A discrete cell approach for modeling single-phase flow in packed beds was analyzed by considering the

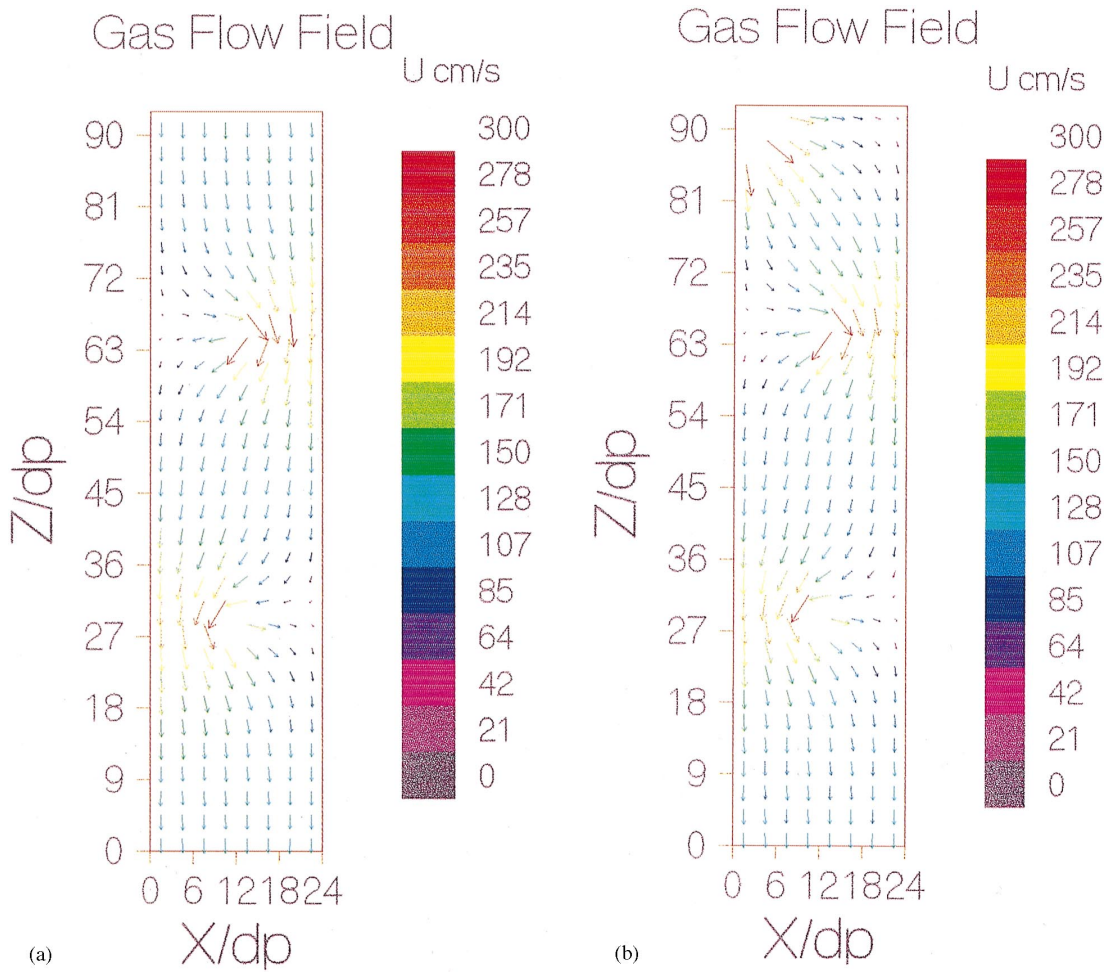

Fig. 13. (a) Interstitial velocity field in a packed bed with two internal obstacles and gas uniform feed from the top at a superficial velocity of 0.5 m/s ($Re' = 28.5$) ($U_0 = 120.5$ cm/s) (velocity vector plotting). (b) Interstitial velocity field in a packed bed with side gas feed and internal obstacles. Inlet gas mean superficial velocity: 0.5 m/s ($Re' = 28.5$) ($U_0 = 120.5$ cm/s) (point source inlet from left side, inlet point superficial velocity is of 4.0 m/s) (*velocity vector plotting*).

contributions of the individual terms in the equation for the rate of energy dissipation. The inertial term in the energy dissipation rate per unit cell is negligible compared to the kinetic term and viscous term except in the regions of structural obstacles. Even in the presence of obstacles the overall inertial term in the total energy dissipation rate is still not important. Reynolds stress term can be ignored due to negligible contribution of this term to cell-scale (i.e. particle diameter scale) fluid velocity distribution. DCM can also be applied for liquid up-flow prediction and gas flow at high operating pressure. A numerical comparison study based on DCM and CFDLIB approaches for the non-parallel flow field has been carried out to verify the DCM approach which rests on the assumption that flow is governed by the minimum rate of total energy dissipation in packed beds. A reasonable agreement between predictions of these two methods is achieved over a wide range of Reynolds numbers for gas flow. It was found that the local superficial velocities track the local bed porosity well. Lower flow resistance produces higher local superficial velocity. The cell superficial velocity with respect to the cross-sectionally averaged superficial velocity varies in the range of 0.8–1.2 for the case considered in this study.

It is not our intent to advocate the use of DCM instead of CFD. The purpose of this study was to indicate that the model so frequently used by engineers, which is based on minimization of the total rate of energy dissipation, indeed works for flows in packed beds in the sense that it provides acceptable solutions of engineering accuracy. The method is relatively simple to use and contains only those physical terms that are deemed important in a particular situation. Using the Ergun equation to describe the pressure drop velocity relation at the cell level is apparently successful enough in describing flows in packed beds for a wide range of Reynolds numbers, fluid densities and velocities. This is the main message of this

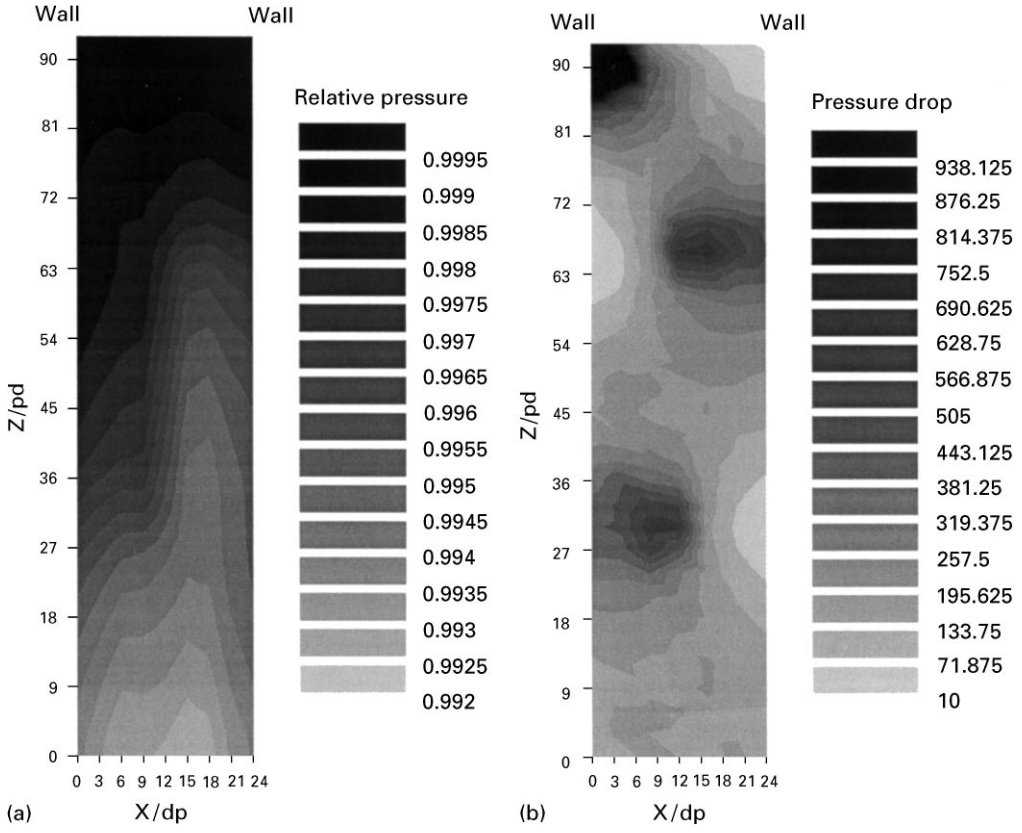

Fig. 14. (a) Pressure field in a packed bed with two internal obstacles and gas uniform feed from the top at a superficial velocity of 0.5 m/s ($Re' = 28.5$). (The relative values of pressure with respect to the inlet operating pressure are plotted.) (b) Dimensionless pressure drop in a packed bed with two internal obstacles and a gas point feed from left side at an equivalent feed superficial velocity of 0.5 m/s ($Re' = 28.5$) (dimensionless pressure drop, $\psi_G = (1/\rho_G g)(\Delta P/\Delta Z)$ is plotted).

paper. It should also be clear that our intent was not to obtain the refined more precise flow field in the presence of internal obstacles in the packed beds, which could be done by local mesh refinement in direct numerical simulation (DNS), but rather to describe the gross flow pattern, which is of interest for quickly evaluating packed-bed reactor performance, at the same level of discretization via DCM and CFD. Only such comparisons are reported.

An agreeable comparison of numerical simulations (DCM and CFDLIB) and experimental velocity data inside a bed is achieved both qualitatively and quantitatively. Additional experimental efforts in obtaining the experimental data of multi-dimensional porosity and fluid velocity distributions are needed to further verify these numerical models and enhance our understanding of flow distribution within beds with complex internal structural non-uniformities.

Acknowledgements

The authors would like to acknowledge the support provided by the industrial sponsors of the Chemical Reaction Engineering Laboratory (CREL) and to thank Dr. R. A. Holub for providing the original version of the DCM code.

Appendix A

The detail derivation of Eq. (4) was given in Holub (1990), and rests on the macroscopic mechanical energy balance. Here we give the main steps of these derivations. For the jth cell, the rate of energy dissipation in $X - Z$ coordinates can be expressed by

$$\sum_{i=1}^{2}\left\{\frac{1}{2}\left(\rho\left(\frac{V}{\varepsilon}\right)^2\left(\frac{V}{\varepsilon}\right)\right)s_i + P\left(\frac{V}{\varepsilon}\right)s_i + \hat{\Phi}\left(\rho\left(\frac{V}{\varepsilon}\right)\right)s_i\right\}_{j,in}$$

$$-\sum_{i=1}^{2}\left\{\left(\rho\left(\frac{V}{\varepsilon}\right)^2\left(\frac{V}{\varepsilon}\right)\right)s_i + P\left(\frac{V}{\varepsilon}\right)s_i + \hat{\Phi}\left(\rho\left(\frac{V}{\varepsilon}\right)\right)s_i\right\}_{j,\mathrm{out}}$$

$$-\left(\frac{E}{\varepsilon}\right)_{V,j} = 0, \tag{A.1}$$

where the superficial velocity (V_j) and the corresponding energy dissipation rate for the cell ($E_{V,j}$) are used. Rearrangement of Eq. (A.1), by substituting the expression for the area for each cell interface, yields

$$\begin{aligned} E_{V,j} = \frac{\rho}{2}\Bigg\{ & \frac{1}{\varepsilon_j^2}(V_X^3 S_X - V_{X+\Delta X}^3 S_{X+\Delta X})_j \\ & + \frac{1}{\varepsilon_j^2}(V_Z^3 S_Z - V_{Z+\Delta Z}^3 S_{Z+\Delta Z})_j \Bigg\} \\ & + \{(P_X V_{X,j} S_X - P_{X+\Delta X} V_{X+\Delta X,j} S_{X+\Delta X}) \\ & + (P_Z V_{Z,j} S_Z - P_{Z+\Delta Z} V_{Z+\Delta Z,j} S_{Z+\Delta Z})\} \\ & + \{(\hat{\Phi}_X \rho V_{X,j} S_X - \hat{\Phi}_{X+\Delta X} \rho V_{X+\Delta X,j} S_{X+\Delta X}) \\ & + (\hat{\Phi}_Z \rho V_{Z,j} S_Z - \hat{\Phi}_{Z+\Delta Z} \rho V_{Z+\Delta Z,j} S_{Z+\Delta Z})\}. \end{aligned} \tag{A.2}$$

The difference in potential energy terms (ΔE_P, Eq. (A.3)) (shown as the last two terms in Eq. (A.2)) can be considered negligible ($\Delta E_P \approx 0$) for gas flow at normal or low pressure since the gravitational force on the gas is very small:

$$\begin{aligned} \Delta E_P = \{ & (\hat{\Phi}_X \rho V_{X,j} S_X - \hat{\Phi}_{X+\Delta X} \rho V_{X+\Delta X,j} S_{X+\Delta X}) \\ & + (\hat{\Phi}_Z \rho V_{Z,j} S_Z - \hat{\Phi}_{Z+\Delta Z} \rho V_{Z+\Delta Z,j} S_{Z+\Delta Z})\} \cong 0. \end{aligned} \tag{A.3}$$

The pressure terms at each cell interface (e.g. P_Z and $P_{Z+\Delta Z}$), however, can be considered to be equal to the pressure at the cell center plus the pressure gradient between the center and the interface. For the Z direction, as an example, the desired relationships can be written as follows:

$$P_Z = P_{cZ} + \left(-\frac{\Delta P}{\Delta Z} \right)_{Z+\Delta Z} \frac{\Delta Z}{2}, \tag{A.4}$$

$$P_{Z+\Delta Z} = P_{cZ} - \left(-\frac{\Delta P}{\Delta Z} \right)_{Z+\Delta Z} \frac{\Delta Z}{2}. \tag{A.5}$$

Rearranging Eq. (A.2), by substituting Eqs. (A.3)–(A.5), gives

$$\begin{aligned} E_{V,j} = \frac{\rho}{2}\Bigg\{ & \frac{1}{\varepsilon_j^2}(V_X^3 S_X - V_{X+\Delta X}^3 S_{X+\Delta X})_j \\ & + \frac{1}{\varepsilon_j^2}(V_Z^3 S_Z - V_{Z+\Delta Z}^3 S_{Z+\Delta Z})_j \\ & + P_{CX}(V_{X,j} S_X - V_{X+\Delta X,j} S_{X+\Delta X}) \\ & + P_{CZ}(V_{Z,j} S_Z - V_{Z+\Delta Z,j} S_{Z+\Delta Z}) \\ & + \frac{\mathrm{Vol}_j}{2}\Bigg\{\Bigg(\left(-\frac{\Delta P}{\Delta X} \right)_X V_{X,j} \\ & + \left(-\frac{\Delta P}{\Delta X} \right)_{X+\Delta X} V_{X+\Delta X,j}\Bigg) \\ & + \Bigg(\left(-\frac{\Delta P}{\Delta Z} \right)_Z V_{Z,j} + \left(-\frac{\Delta P}{\Delta Z} \right)_{Z+\Delta Z} V_{Z+\Delta Z,j}\Bigg)\Bigg\}. \end{aligned} \tag{A.6}$$

For each cell, we can write the Eq. (A.7) based on the mass balance as

$$\begin{aligned} & (V_{X,j} S_X - V_{X+\Delta X,j} S_{X+\Delta X}) \\ & \quad + (V_{Z,j} S_Z - V_{Z+\Delta Z,j} S_{Z+\Delta Z}) = 0. \end{aligned} \tag{A.7}$$

Since the magnitudes of P_{CZ} and P_{CX} have to be the same at the central point of the cell j, the substitution of the mass balance equation (A.7) into Eq. (A.6) eliminates the central pressure term. To completely eliminate the pressure terms from Eq. (A.6), the body force terms, represented by the pressure gradient, can be replaced by an appropriate drag force model which relates pressure drop to the local superficial velocity. In this work, a specially abbreviated form of the Ergun (1952) equation for each coordinate direction (X and Z) will be used to simplify the equations. For example, for the Z direction, we have

$$\left(-\frac{1}{\rho}\frac{\Delta P}{\Delta Z} \right)_Z = f_{1,j} V_{Z,j} + f_{2,j} V_{Z,j} |V_{Z,j}|, \tag{A.8}$$

where the pressure loss per unit cell is caused by simultaneous viscous and kinetic energy losses. The resulting expression for calculating the energy dissipation rate per unit cell can be obtained, as shown by Eq. (4), and the total energy dissipation rate for the entire bed is then obtained by the summation of Eq. (4) over all the cells (see Eq. (8)).

References

Benenati, R. F., & Brosilow, C. B. (1962). Void fraction distribution in beds of spheres. *A.I.Ch.E. Journal*, *8*, 359–361.

Bey, O., & Eigenberger, G. (1997). Fluid flow through catalyst filled tubes. *Chemical Engineering Science*, *52*, 1365–1376.

Berninger, R., & Vortmeyer, D. (1987a). Die Umströmung von Hindernissen in Schüttungen. *Chemie-Ingenienr-Technik*, *59*, 224.

Berninger, R., & Vortmeyer, D. (1987b). Der Einfluß von Versperrung auf das reaktionstechnische Verhalten eines adiabaten Festbettreaktors. *Chemi-Ingenienr-Technik*, *60*, 1052.

Cheng, Zhen-Min, & Yuan, Wei-Kang. (1997). Estimating Radial velocity of fixed beds with low tube-to-particle diameter ratios. *A.I.Ch.E. Journal*, *43*, 1319–1324.

Choudhary, M., Propster, M., & Szekely, J. (1976). On the importance of the inertial terms in the modeling of flow maldistribution in packed beds. *A.I.Ch.E. Journal*, *22*, 600–603.

Cohen, Y., & Metzner, A. B. (1981). Wall effects in laminar flow of fluids through packed beds. *A.I.Ch.E. Journal*, *27*, 705–715.

Daszkowski, T., & Eigenberger, G. (1992). A revaluation of fluid flow, heat transfer and chemical reaction in catalyst filled tubes. *Chemical Engineering Science*, *47*, 2245–2250.

Delmas, H., & Froment, G. F. (1988). A simulation model accounting for structural radial nonuniformities in fixed bed reactors. *Chemical Engineering Science*, *43*, 2281–2287.

Ergun, S. (1952). Fluid flow through packed columns. *Chemical Engineering Progress*, *48*, 88–94.

Fluent 4.4 (1997). User's guide, (2nd ed.). NH, USA: Fluent Inc.

Haughey, D. P., & Beveridge, G. S. G. (1969). Structural properties of packed beds: A review. *Canadian Journal of Chemical Engineering*, *47*, 130.

Holub, R. A. (1990). *Hydrodynamics of trickle bed reactors*. Ph.D. thesis, Washington University in St. Louis, MO, USA.

Hyre, M., & Glicksman, L. (1997). Brief communication on the assumption of minimization energy dissipation in circulating fluidized beds. *Chemical Engineering Science*, *14*, 2435–2438.

Ishii, M. (1975). *Thermo-fluid dynamic theory of two-phase flow*. Direction des Etudes et Researches d'Electricité de France, EYROLLES.

Ishii, H., Nakajima, T., & Horio, M. (1989). The clustering annular flow model of circulating fluidized beds. *Journal of Chemical Engineering of Japan*, *22*, 484–490.

Jaynes, E. T. (1980). The minimum entropy production principle. *Annual Review of Physics and Chemistry*, *31*, 579.

Johnson, G. W., & Kapner, R. S. (1990). The dependence of axial dispersion on non-uniform flows in beds of uniform packing. *Chemical Engineering Science*, *45*, 3329.

Johnson, N. L., Kashiwa, B. A., & Vander Heyden, W. B. (1997). Multi-phase flows and particle Methods (Part-B). *The fifth annual conference of the computational fluid dynamics society of Canada*, May 28–29, British Columbia, Canada.

Jolls, K. R., & Hanratty, T. J. (1969). Use of electochemical techniques to study mass transfer rates and local skin friction to a sphere in dumped bed. *A.I.Ch.E. Journal*, *15*, 199–205.

Joseph, D. D. (1998). Flow induce microstructure and direct simulation of liquid–solid flow. *Annual A.I.Ch.E. meeting, PTF topical conference*, Miami Beach, FL, USA.

Kashiwa, B. A., Padial, N. T., Rauenzahn, R. M., & Vander Heyden, W. B. (1994). A cell centered ICE method for multiphase flow simulations. *ASME symposium on numerical methods for multiphase flows*, Lake Tahoe, Nevada.

Kitaev, B. et al., (1975) Investigation of the aerodynamics in packed metallurgical furnaces with tuyere wind entry. *BFA symposium*, Wollongong, Australia.

Kumar, S. (1995). Simulation of multiphase flow system using CFDLIB code. *CREL annual meeting workshop*, St. Louis, MO, USA.

Latifi, M. A., Midoux, N., & Storck, A. (1989). The use of microelectrodes in the study of the flow regimes in packed bed reactor with single phase liquid flow. *Chemical Engineering Science*, *44*, 2501–2508.

Lerou, J. J., & Froment, G. F. (1977). Velocity, temperature, and conversion profiles in fixed bed catalyst reactors. *Chemical Engineering Science*, *32*, 853–861.

Li, J., Tung, Y., & Kwauk, M. (1988). Energy transport and regime transition in particle-fluid two-phase flow. In P. Basu, & J. F. Large, *Circulating fluidized bed technology II* (p. 75). Oxford, UK: Pergamon.

Li, J., Reh, L., & Kwauk, M. (1990). Application of the principle of energy minimization to the fluid-dynamics of circulating Fluidized Beds. *Proceedings of the Third international conference on circulating fluidized beds*, Nagoya, Japan.

MacDonald, I. F., El-Sayed, M. S., Mow, K., & Dullien, F. A. (1979). Flow through porous media-the Ergun equation revisited. *Industrial and Engineering Chemistry, Fundamentals*, *18*, 199.

McGreavy, C., Foumeny, E. A., & Javed, K. H. (1986). Characterization of transport properties for fixed bed in terms of local bed structure and flow distribution. *Chemical Engineering Science*, *36*, 787–797.

Morales, M., Spinn, C. W., & Smith, J. M. (1951). Velocities and thermal conductivities in packed beds. *Industrial and Engineering Chemistry Research*, *43*, 225–232.

Nijemeisland, M., Logtenberg, S. A., & Dixon, A. G. (1998). CFD studies of wall-region fluid flow and heat transfer in a fixed bed reactor. *A.I.Ch.E. annual meeting*, paper 311f, Miami Beach, FL, USA.

Peurrung, L. M., Rashidi, M., & Kulp, T. J. (1995). Measurement of porous medium velocity fields and their volumetric averaging characteristics using particle tracking velocimetry. *Chemical Engineering Science*, *50*, 2243–2253.

Schwartz, C. E., & Smith, J. M. (1953). Flow distribution in packed beds. *Industrial and Engineering Chemistry*, *45*, 1205–1218.

Song, M., Yin, F. H., Nandakumar, K., & Chuang, K. T. (1998). A three-dimension model for simulating the maldistribution of liquid flow in random packed beds. *Canadian Jouranl of Chemical Engineering*, *76*, 161–166.

Stanek, V. (1994). *Fixed bed operations: Flow distribution and efficiency*, Series in Chemical Engineering. Chichester: Ellis Horwood.

Stanek, V., & Szekely, J. (1972). The effect of non-uniform porosity in causing flow maldistribution in isothermal packed beds. *Canadian Journal of Chemical Engineering*, *50*, 9–14.

Stanek, V., & Szekely, J. (1973). Flow maldistribution in two dimensional packed beds, Parts II: The behavior of non-isothermal systems. *Canadian Journal of Chemical Engineering*, *51*, 22–30.

Stanek, V., & Szekely, J. (1974). Three-dimensional flow of fluids through nonuniform packed beds. *A.I.Ch.E. Journal*, *20*, 974–980.

Stephenson, J. L., & Stewart, W. E. (1986). Optical measurements of porosity and fluid motion in packed beds. *Chemical Engineering Science*, *41*, 2161–2170.

Subagyo, Standish, N., & Brooks, G. A. (1998). A new model of velocity distribution of a single-phase fluid flowing in packed beds. *Chemical Engineering Science*, *53*, 1375–1385.

Szekely, J., & Poveromo, J. J. (1975). Flow maldistribution in Packed Beds: A comparison of measurements with predictions. *A.I.Ch.E. Journal*, *21*, 769.

Tory, E. M., Church, B. H., Tam, M. K., & Ratner, M. (1973). Simulated random packing of equal spheres. *Canadian Journal of Chemical Engineering*, *51*, 484–493.

Volkov, S. A., Reznikov, V. I., Khalilov, K. F., Zel'vensky, Yu, V., & Sakodynsky, K. I. (1986). Nonuniformity of packed beds and its influence on longitudinal dispersion. *Chemical Engineering Science*, *41*, 389–397.

Vortmeyer, D., & Schuster, J. (1983). Evaluation of steady flow profiles in rectangular and circular packed beds by a variational method. *Chemical Engineering Science*, *38*, 1691–1699.

Vortmeyer, D., & Winter, R. P. (1984). Improvements in reactor analysis incorporating porosity and velocity profiles. *German Chemical Engineering*, *7*, 19.

Ziolkowska, I., & Ziolkowski, D. (1993). Modeling of gas interstitial velocity radial distribution over a cross-section of a tube packed with a granular catalyst bed. *Chemical Engineering Science*, *48*, 3283–3292.